Report on

Scalar and tensor structures in $\eta_c\eta_c$ and $J/\psi J/\psi$ scattering from lattice QCD

Dr. Geng Li
ligeng@ihep.ac.cn

October 11, 2025

Institute of High Energy Physics (IHEP), Chinese Academy of Sciences (CAS)

Based on: arXiv:2505.24213 (short), arXiv:2505.23220 (detailed)

Co-authors

Dr. Geng Li (李更)

Dr. Chun-Jiang Shi (施春江)

Prof. Ying Chen (陈莹)

Dr. Wei Sun (孙玮)

Figure 1: Co-authors in Institute of High Energy Physics (IHEP), CAS

Outline

Motivation

- In 2003, Belle[1] proposed first Tetraquark candidate of X(3872);
- In 2020, LHCb[2] discovered all-charm Tetraquark candidate of X(6900) ($T_{cc\bar{c}\bar{c}}(6900)$ on PDG);
- In 2022, ATLAS[3] also observed X(6900) and lower broad structure;

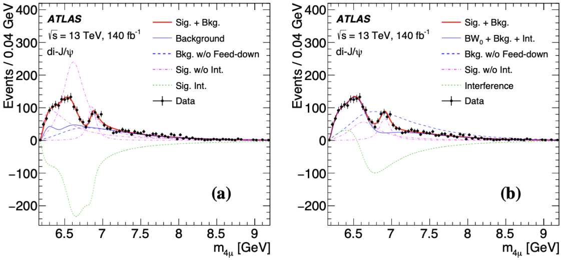

di-J/ψ	model A	model B
m_0	$6.41 \pm 0.08^{+0.08}_{-0.03}$	$6.65 \pm 0.02^{+0.03}_{-0.02}$
Γ_0	$0.59 \pm 0.35^{+0.12}_{-0.20}$	$0.44 \pm 0.05^{+0.06}_{-0.05}$
m_1	$6.63 \pm 0.05^{+0.08}_{-0.01}$	—
Γ_1	$0.35 \pm 0.11^{+0.11}_{-0.04}$	
m_2	$6.86 \pm 0.03^{+0.01}_{-0.02}$	$6.91 \pm 0.01 \pm 0.01$
Γ_2	$0.11 \pm 0.05^{+0.02}_{-0.01}$	$0.15 \pm 0.03 \pm 0.01$
$\Delta s/s$	$\pm 5.1\%^{+8.1\%}_{-8.9\%}$	—
$J/\psi+\psi(2S)$	model α	model β
m_3	$7.22 \pm 0.03^{+0.01}_{-0.04}$	$6.96 \pm 0.05 \pm 0.03$
Γ_3	$0.09 \pm 0.06^{+0.06}_{-0.05}$	$0.51 \pm 0.17^{+0.11}_{-0.10}$
$\Delta s/s$	$\pm 21\%^{+25\%}_{-15\%}$	$\pm 20\% \pm 12\%$

Figure 2: ATLAS 2022

[1] Phys.Rev.Lett. 91 (2003) 262001
[2] Sci.Bull. 65 (2020) 23, 1983-1993
[3] Phys.Rev.Lett. 131 (2023)151902

Experiments

- In 2023, CMS[4] reported a Tetraquark family of X(6600), X(6900) and X(7300);

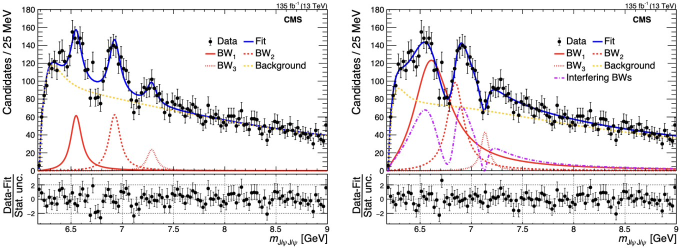

		BW_1	BW_2	BW_3
No interference	m (MeV)	$6552 \pm 10 \pm 12$	$6927 \pm 9 \pm 4$	$7287^{+20}_{-18} \pm 5$
	Γ (MeV)	$124^{+32}_{-26} \pm 33$	$122^{+24}_{-21} \pm 18$	$95^{+59}_{-40} \pm 19$
	N	470^{+120}_{-110}	492^{+78}_{-73}	156^{+64}_{-51}
Interference	m (MeV)	6638^{+43+16}_{-38-31}	6847^{+44+48}_{-28-20}	7134^{+48+41}_{-25-15}
	Γ (MeV)	$440^{+230+110}_{-200-240}$	191^{+66+25}_{-49-17}	97^{+40+29}_{-29-26}

Figure 3: CMS 2023

[4] Phys.Rev.Lett. 132 (2024) 11, 111901

Motivation

- LHCb, ATLAS, CMS all observed structures around 6600 and 6900 MeV in the invariant mass spectrum. For $X(6600)$, the mass is measured as around $6.5 - 6.6$ GeV, and the width is measured as several hundred MeV (differences depending on fitting models);
- In April 2025, CMS[5] reported $J^{PC} = 2^{++}$ match the expected values by angular analysis techniques;
- Lattice QCD: from first principle, avoid introducing effective coupling constants. For now, only one LQCD work[6] calculated the low-energy S-wave scattering at zero relative momentum (indicate repulsive interaction near the threshold);
- In this study, we first calculated the lattice energy level spectrum based on the meson molecule model. And firstly find a resonance near 6.54 GeV with width ~ 540 MeV in the 2^{++} S-wave $J/\psi J/\psi$ channel;

[5] Submit to Nature

[6] Eur.Phys.J.C 85 (2025) 4, 458

Lattice simulation

Correlation function from LQCD

- The Green's function in path integral formulation

$$\langle\Omega|\hat{T}\mathcal{O}(x_1,x_2,x_3,\ldots)|\Omega\rangle = \frac{1}{Z}\int \mathcal{D}A_\mu\bar{\psi}\mathcal{D}\psi\mathcal{O}(x_1,x_2,x_3,\ldots)e^{i\int d^4x\mathcal{L}_{QCD}},$$

- In discrete space and on specific configurations

$$\langle\Omega|\hat{T}\mathcal{O}[\psi_q,\bar{\psi}_q,U]|\Omega\rangle = \frac{1}{Z_E}\int DU\prod_q\left[\det M[U,m_q]\right]e^{-S_G[U]}\mathcal{O}\left[S_q[U],U\right] \equiv \langle\mathcal{O}[S_q[U],U]\rangle,$$

- Anisotropic lattice with two sizes, two sea pion masses, where $\vec{k} = 2\pi\,\vec{n}/L_s$

IE	$N_s^3\times N_t$	m_π(MeV)	$m_\pi L_s$	M_{η_c}(MeV)	$M_{J/\psi}$(MeV)	a_t^{-1}(GeV)	ξ_{η_c}	$\xi_{J/\psi}$	N_V	$N_{\rm cfg}$
L12M420	$12^3\times96$	426(4)	~3.4	2995.97(66)	3088.50(86)	7.219	5.100(6)	5.087(8)	170	400
L16M420	$16^3\times128$	417(6)	~4.6	2995.25(34)	3087.14(48)	7.219	5.081(8)	5.063(10)	120	400
L12M250	$12^3\times96$	~250	~2.1	2995.67(69)	3081.66(91)	7.276	5.148(7)	5.118(7)	170	400
L16M250	$16^3\times128$	250(3)	~2.8	2998.32(34)	3085.29(45)	7.276	5.120(9)	5.103(11)	120	400

- Distillation method: repeated use of the perambulator;

0^{++} Operator set

- ${}^1S_0$ $\mathcal{O}_{\eta_c\eta_c}(n^2(k)) = \sum_{R\in O} \mathcal{O}_{\eta_c}(R\vec{k})\mathcal{O}_{\eta_c}(-R\vec{k})$

$\mathcal{O}_{\eta_c\eta_c}(n^2)$	S-wave Operators
$n^2=0$	$[\bar{c}\gamma^5 c](0,0,0)\times[\bar{c}\gamma^5 c](0,0,0)$
$n^2=1$	$[\bar{c}\gamma^5 c](-1,0,0)\times[\bar{c}\gamma^5 c](1,0,0)+[\bar{c}\gamma^5 c](0,-1,0)\times[\bar{c}\gamma^5 c](0,1,0)+[\bar{c}\gamma^5 c](0,0,-1)\times[\bar{c}\gamma^5 c](0,0,1)$ $+[\bar{c}\gamma^5 c](0,0,1)\times[\bar{c}\gamma^5 c](0,0,-1)+[\bar{c}\gamma^5 c](0,1,0)\times[\bar{c}\gamma^5 c](0,-1,0)+[\bar{c}\gamma^5 c](1,0,0)\times[\bar{c}\gamma^5 c](-1,0,0)$
$n^2=2$	$[\bar{c}\gamma^5 c](-1,-1,0)\times[\bar{c}\gamma^5 c](1,1,0)+[\bar{c}\gamma^5 c](-1,0,-1)\times[\bar{c}\gamma^5 c](1,0,1)+[\bar{c}\gamma^5 c](-1,0,1)\times[\bar{c}\gamma^5 c](1,0,-1)$ $+[\bar{c}\gamma^5 c](-1,1,0)\times[\bar{c}\gamma^5 c](1,-1,0)+[\bar{c}\gamma^5 c](0,-1,-1)\times[\bar{c}\gamma^5 c](0,1,1)+[\bar{c}\gamma^5 c](0,-1,1)\times[\bar{c}\gamma^5 c](0,1,-1)$ $+[\bar{c}\gamma^5 c](0,1,-1)\times[\bar{c}\gamma^5 c](0,-1,1)+[\bar{c}\gamma^5 c](0,1,1)\times[\bar{c}\gamma^5 c](0,-1,-1)+[\bar{c}\gamma^5 c](1,-1,0)\times[\bar{c}\gamma^5 c](-1,1,0)$ $+[\bar{c}\gamma^5 c](1,0,-1)\times[\bar{c}\gamma^5 c](-1,0,1)+[\bar{c}\gamma^5 c](1,0,1)\times[\bar{c}\gamma^5 c](-1,0,-1)+[\bar{c}\gamma^5 c](1,1,0)\times[\bar{c}\gamma^5 c](-1,-1,0)$
$n^2=3$	$[\bar{c}\gamma^5 c](-1,-1,-1)\times[\bar{c}\gamma^5 c](1,1,1)+[\bar{c}\gamma^5 c](-1,-1,1)\times[\bar{c}\gamma^5 c](1,1,-1)+[\bar{c}\gamma^5 c](-1,1,-1)\times[\bar{c}\gamma^5 c](1,-1,1)$ $+[\bar{c}\gamma^5 c](-1,1,1)\times[\bar{c}\gamma^5 c](1,-1,-1)+[\bar{c}\gamma^5 c](1,-1,-1)\times[\bar{c}\gamma^5 c](-1,1,1)+[\bar{c}\gamma^5 c](1,-1,1)\times[\bar{c}\gamma^5 c](-1,1,-1)$ $+[\bar{c}\gamma^5 c](1,1,-1)\times[\bar{c}\gamma^5 c](-1,-1,1)+[\bar{c}\gamma^5 c](1,1,1)\times[\bar{c}\gamma^5 c](-1,-1,-1)$
$n^2=4$	$[\bar{c}\gamma^5 c](-2,0,0)\times[\bar{c}\gamma^5 c](2,0,0)+[\bar{c}\gamma^5 c](0,-2,0)\times[\bar{c}\gamma^5 c](0,2,0)+[\bar{c}\gamma^5 c](0,0,-2)\times[\bar{c}\gamma^5 c](0,0,2)$ $+[\bar{c}\gamma^5 c](0,0,2)\times[\bar{c}\gamma^5 c](0,0,-2)+[\bar{c}\gamma^5 c](0,2,0)\times[\bar{c}\gamma^5 c](0,-2,0)+[\bar{c}\gamma^5 c](2,0,0)\times[\bar{c}\gamma^5 c](-2,0,0)$
$n^2=5$	$[\bar{c}\gamma^5 c](-2,-1,0)\times[\bar{c}\gamma^5 c](2,1,0)+[\bar{c}\gamma^5 c](-2,0,-1)\times[\bar{c}\gamma^5 c](2,0,1)+[\bar{c}\gamma^5 c](-2,0,1)\times[\bar{c}\gamma^5 c](2,0,-1)$ $+[\bar{c}\gamma^5 c](-2,1,0)\times[\bar{c}\gamma^5 c](2,-1,0)+[\bar{c}\gamma^5 c](-1,-2,0)\times[\bar{c}\gamma^5 c](1,2,0)+[\bar{c}\gamma^5 c](-1,0,-2)\times[\bar{c}\gamma^5 c](1,0,2)$ $+[\bar{c}\gamma^5 c](-1,0,2)\times[\bar{c}\gamma^5 c](1,0,-2)+[\bar{c}\gamma^5 c](-1,2,0)\times[\bar{c}\gamma^5 c](1,-2,0)+[\bar{c}\gamma^5 c](0,-2,-1)\times[\bar{c}\gamma^5 c](0,2,1)$ $+[\bar{c}\gamma^5 c](0,-2,1)\times[\bar{c}\gamma^5 c](0,2,-1)+[\bar{c}\gamma^5 c](0,-1,-2)\times[\bar{c}\gamma^5 c](0,1,2)+[\bar{c}\gamma^5 c](0,-1,2)\times[\bar{c}\gamma^5 c](0,1,-2)$ $+[\bar{c}\gamma^5 c](0,1,-2)\times[\bar{c}\gamma^5 c](0,-1,2)+[\bar{c}\gamma^5 c](0,1,2)\times[\bar{c}\gamma^5 c](0,-1,-2)+[\bar{c}\gamma^5 c](0,2,-1)\times[\bar{c}\gamma^5 c](0,-2,1)$ $+[\bar{c}\gamma^5 c](0,2,1)\times[\bar{c}\gamma^5 c](0,-2,-1)+[\bar{c}\gamma^5 c](1,-2,0)\times[\bar{c}\gamma^5 c](-1,2,0)+[\bar{c}\gamma^5 c](1,0,-2)\times[\bar{c}\gamma^5 c](-1,0,2)$ $+[\bar{c}\gamma^5 c](1,0,2)\times[\bar{c}\gamma^5 c](-1,0,-2)+[\bar{c}\gamma^5 c](1,2,0)\times[\bar{c}\gamma^5 c](-1,-2,0)+[\bar{c}\gamma^5 c](2,-1,0)\times[\bar{c}\gamma^5 c](-2,1,0)$ $+[\bar{c}\gamma^5 c](2,0,-1)\times[\bar{c}\gamma^5 c](-2,0,1)+[\bar{c}\gamma^5 c](2,0,1)\times[\bar{c}\gamma^5 c](-2,0,-1)+[\bar{c}\gamma^5 c](2,1,0)\times[\bar{c}\gamma^5 c](-2,-1,0)$

- ${}^1S_0$ $\mathcal{O}_{\psi\psi} = \sum_{R\in O}\left[\mathcal{O}^1_{\psi}(R\vec{k})\mathcal{O}^1_{\psi}(-R\vec{k})+\mathcal{O}^2_{\psi}(R\vec{k})\mathcal{O}^2_{\psi}(-R\vec{k})+\mathcal{O}^3_{\psi}(R\vec{k})\mathcal{O}^3_{\psi}(-R\vec{k})\right]$, $\mathcal{O}^i_{\psi}=[\bar{c}\gamma^i c]$

2^{++} Operator set

- ${}^5S_2$ $\mathcal{O}^{S\text{-}E(1)}_{\psi\psi} = \sum_{R\in O}\left[\mathcal{O}^1_\psi(R\vec{k})\mathcal{O}^1_\psi(-R\vec{k}) - \mathcal{O}^2_\psi(R\vec{k})\mathcal{O}^2_\psi(-R\vec{k})\right], \mathcal{O}^i_\psi = [\bar{c}\gamma^i c]$
- ${}^1D_2$ $\mathcal{O}^{E(1)}_{\eta_c\eta_c} = \sum_{R\in O} c^{E(1)}_R \mathcal{O}_{\eta_c}(R\vec{k})\mathcal{O}_{\eta_c}(-R\vec{k})$

$\mathcal{O}_{\eta_c\eta_c}(n^2)$	D-wave Operators
$n^2=1$	$-[\bar{c}\gamma^5c](-1,0,0)\times[\bar{c}\gamma^5c](1,0,0) - [\bar{c}\gamma^5c](0,-1,0)\times[\bar{c}\gamma^5c](0,1,0) + 2[\bar{c}\gamma^5c](0,0,-1)\times[\bar{c}\gamma^5c](0,0,1)$ $+2[\bar{c}\gamma^5c](0,0,1)\times[\bar{c}\gamma^5c](0,0,-1) - [\bar{c}\gamma^5c](0,1,0)\times[\bar{c}\gamma^5c](0,-1,0) - [\bar{c}\gamma^5c](1,0,0)\times[\bar{c}\gamma^5c](-1,0,0)$
$n^2=2$	$-[\bar{c}\gamma^5c](-1,-1,0)\times[\bar{c}\gamma^5c](1,1,0) + \frac{1}{2}[\bar{c}\gamma^5c](-1,0,-1)\times[\bar{c}\gamma^5c](1,0,1) + \frac{1}{2}[\bar{c}\gamma^5c](-1,0,1)\times[\bar{c}\gamma^5c](1,0,-1)$ $-[\bar{c}\gamma^5c](-1,1,0)\times[\bar{c}\gamma^5c](1,-1,0) + \frac{1}{2}[\bar{c}\gamma^5c](0,-1,-1)\times[\bar{c}\gamma^5c](0,1,1) + \frac{1}{2}[\bar{c}\gamma^5c](0,-1,1)\times[\bar{c}\gamma^5c](0,1,-1)$ $+\frac{1}{2}[\bar{c}\gamma^5c](0,1,-1)\times[\bar{c}\gamma^5c](0,-1,1) + \frac{1}{2}[\bar{c}\gamma^5c](0,1,1)\times[\bar{c}\gamma^5c](0,-1,-1) - [\bar{c}\gamma^5c](1,-1,0)\times[\bar{c}\gamma^5c](-1,1,0)$ $+\frac{1}{2}[\bar{c}\gamma^5c](1,0,-1)\times[\bar{c}\gamma^5c](-1,0,1) + \frac{1}{2}[\bar{c}\gamma^5c](1,0,1)\times[\bar{c}\gamma^5c](-1,0,-1) - [\bar{c}\gamma^5c](1,1,0)\times[\bar{c}\gamma^5c](-1,-1,0)$
$n^2=4$	$-[\bar{c}\gamma^5c](-2,0,0)\times[\bar{c}\gamma^5c](2,0,0) - [\bar{c}\gamma^5c](0,-2,0)\times[\bar{c}\gamma^5c](0,2,0) + 2[\bar{c}\gamma^5c](0,0,-2)\times[\bar{c}\gamma^5c](0,0,2)$ $+2[\bar{c}\gamma^5c](0,0,2)\times[\bar{c}\gamma^5c](0,0,-2) - [\bar{c}\gamma^5c](0,2,0)\times[\bar{c}\gamma^5c](0,-2,0) - [\bar{c}\gamma^5c](2,0,0)\times[\bar{c}\gamma^5c](-2,0,0)$

- ${}^1D_2$ $\mathcal{O}^{D\text{-}E(1)}_{\psi\psi} = \sum_{R\in O}\left[c^{E(1)}_R\mathcal{O}^1_\psi(R\vec{k})\mathcal{O}^1_\psi(-R\vec{k}) - c^{E(1)}_R\mathcal{O}^2_\psi(R\vec{k})\mathcal{O}^2_\psi(-R\vec{k})\right]$

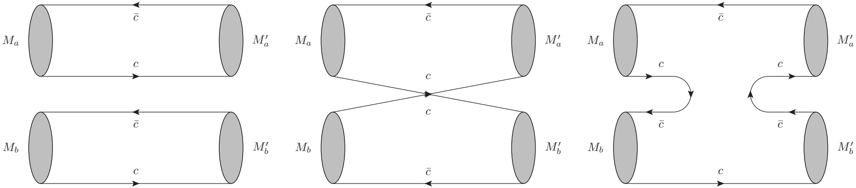

(a) Direct **(b)** Quark rearrangement **(c)** Single annihilation

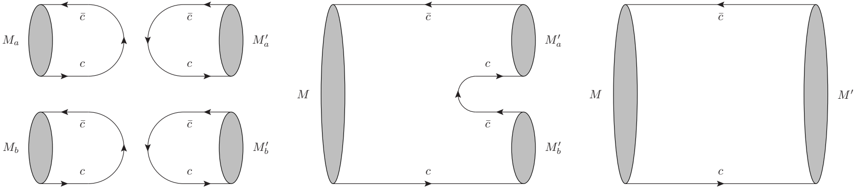

(d) Double annihilation **(e)** $c\bar{c}$ and two-particle operators **(f)** $c\bar{c}$ operator

Figure 4: Schematic illustrations of quark Wick contractions.

Correlation matrix for 0^{++}

- For each operator set we calculate the correlation matrix with $\mathcal{O} \in S_{0(2)}$.

$$C_{\alpha\beta}(t) = \langle \mathcal{O}_\alpha(t)\mathcal{O}^\dagger_\beta(0)\rangle.$$

- Solving the generalized eigenvalue problem (GEVP) to the correlation matrix $C_{\alpha\beta}(t)$

$$C_{\alpha\beta}(t)v^{(n)}_\beta = \lambda^{(n)}(t,t_0)C_{\alpha\beta}(t_0)v^{(n)}_\beta,$$

- We introduce the following weight function to visualize the the correlation strength,

$$w_{\alpha\beta}(t) = \frac{C_{\alpha\beta}(t)}{\sqrt{C_{\alpha\alpha}(t)C_{\beta\beta}(t)}}.$$

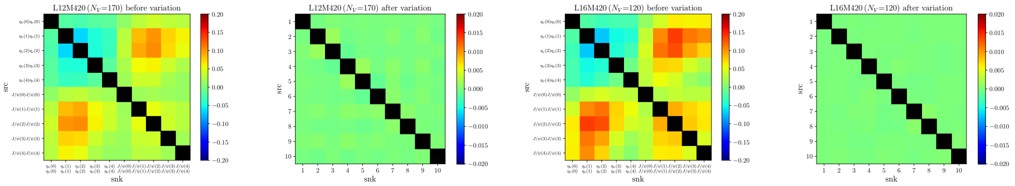

Figure 5: Correlation matrix $\tilde{C}(t)$ at $t = 20\ (35)\ a_t$ on the L12M420 and L16M420 ensembles, where the operator is written in the form of $\mathcal{O}_M(n^2)\mathcal{O}_M(n^2)$.

Correlation matrix for 2^{++}

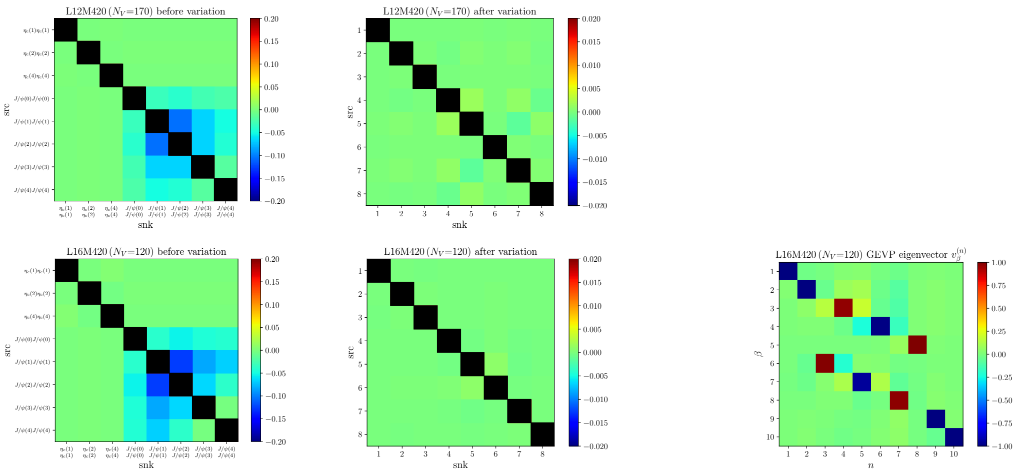

Figure 6: Correlation matrix $\tilde{C}(t)$ at $t = 20\,(35)\,a_t$ on the L12M420 (top) and L16M420 (bottom) ensembles, where the operator is written in the form of $\mathcal{O}_M(n^2)\mathcal{O}_M(n^2)$. The left and right panels show the matrices before and after the variation analysis, respectively.

Fit lattice energy levels

For (I), the correlation function can be parameterized as

$$C(t) = W_1 \cosh\left[E_{(h_1 h_2)}(\tau - \frac{T}{2})\right] + W_2 \cosh\left[\left(E_{h_1} - E_{h_2}\right)(\tau - \frac{T}{2})\right] + W' \cosh\left[E'(\tau - \frac{T}{2})\right],$$

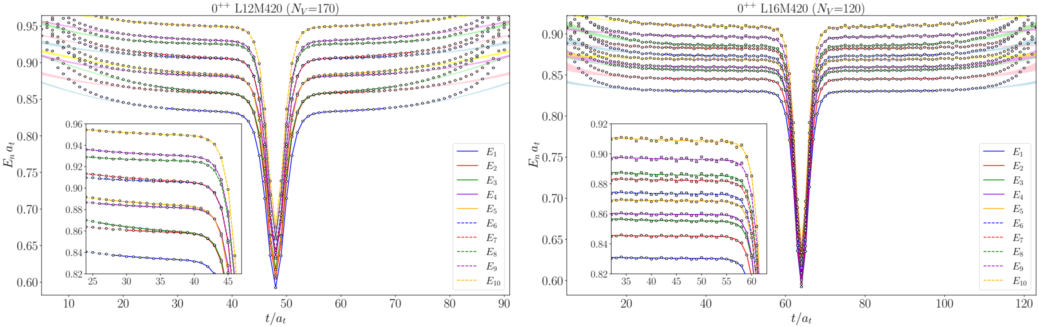

Figure 7: Fit energy levels with three-state model.

For (II), the following ratio is constructed to describe scattering correlation

$$R(t) = \frac{C_{(4)}(t/a_t) - C_{(4)}(t/a_t + 1)}{\left[C_{(2)}(t/a_t)\right]^2 - \left[C_{(2)}(t/a_t + 1)\right]^2}, \quad R(t) = A_R \frac{\sinh\left[E^{(4)}(t/a_t - 1)\right]}{\sinh\left[2m_\pi(t/a_t - 1)\right]}.$$

Two methods

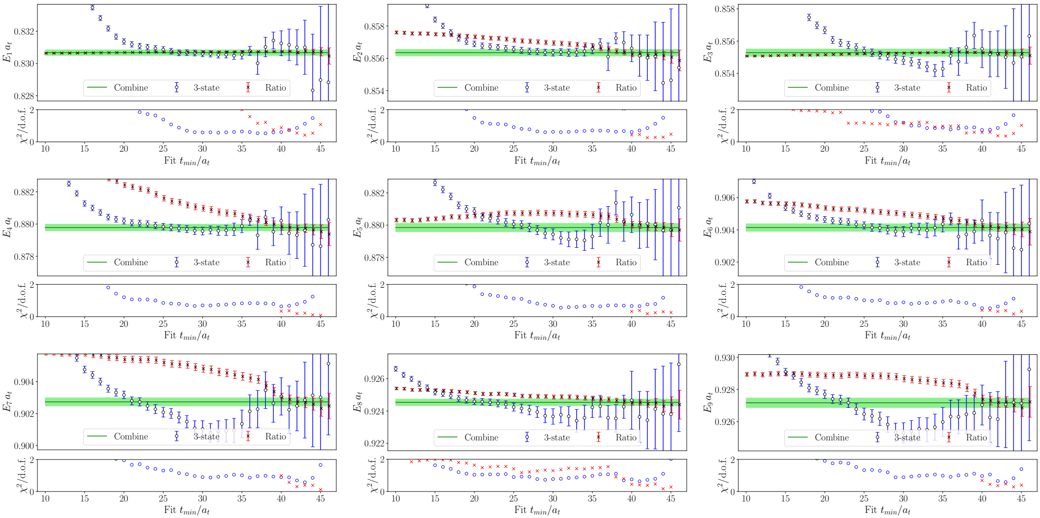

Figure 8: Fit energy levels on L12M420 with method (I) (blue) and method (II) (red).

Energy level spectrum

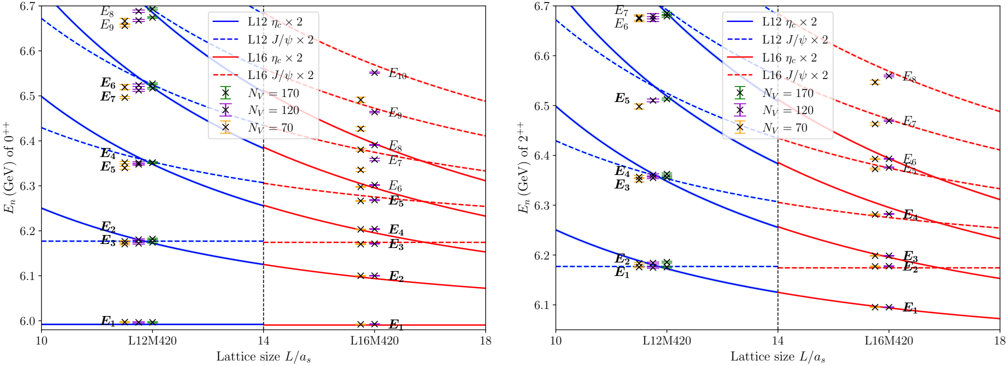

Figure 9: Energy level spectrum for 0^{++} and 2^{++} system.

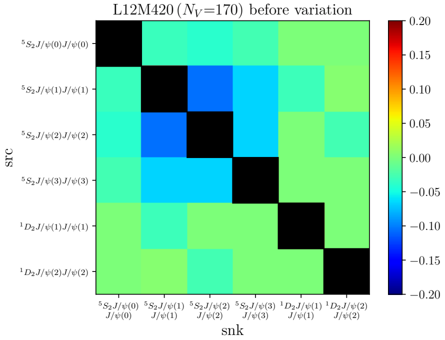

E_n of $J/\psi J/\psi$	L12 non-int	L12 E_n	L12 E_n'''
$^5S_2$ ($n^2 = 0$)	6.1770(17)	**6.1858(17)**	6.1855(17)
$^5S_2$ ($n^2 = 1$)	6.3532(22)	**6.3626(20)**	6.3634(20)
$^1D_2$ ($n^2 = 1$)	6.3532(22)	-	6.3528(20)
$^5S_2$ ($n^2 = 2$)	6.5247(27)	**6.5129(20)**	6.5147(19)
$^1D_2$ ($n^2 = 2$)	6.5247(27)	-	6.5304(19)
$^5S_2$ ($n^2 = 3$)	6.6918(31)	6.6849(24)	6.6902(19)

Scattering analysis

Lüscher's fromalism

- The state-of-arts technique: Lüscher's formalism,

$$\det[\mathbf{I} + i\rho(E_{\rm cm})\mathbf{t}(E_{\rm cm})(\mathbf{I} - i\mathcal{M}(E_{\rm cm}, L)] = 0,$$

- The unitarity condition of S-matrix requires Im $\mathbf{t}^{-1} = -i\rho$, so after the analytical continuing to the complex plane of the invariant mass squared s, the K-matrix gives the parameterization

$$\mathbf{t}^{-1}(s) = \mathbf{K}^{-1}(s) - i\rho(s),$$

- For the S-wave single-channel two-body scattering, the scattering amplitude t can be expressed in terms of the scattering phase δ_0 as

$$t(s) = \frac{8\pi\sqrt{s}}{k\cot\delta_0(k) - ik},$$

- With the convention of the phase space factor $\rho = \frac{1}{8\pi}\frac{k}{\sqrt{s}}$, Lüscher's quantization condition is

$$k\cot\delta_0(k) = k\mathcal{M}_{0000}(q^2) = \frac{2}{L\sqrt{\pi}}\mathcal{Z}_{00}(1, q^2), \text{ where Zeta function } \mathcal{Z}_{00} = \frac{1}{\sqrt{4\pi}}\sum_{\vec{n}\in Z^3}\frac{1}{\vec{n}^2 - q^2}.$$

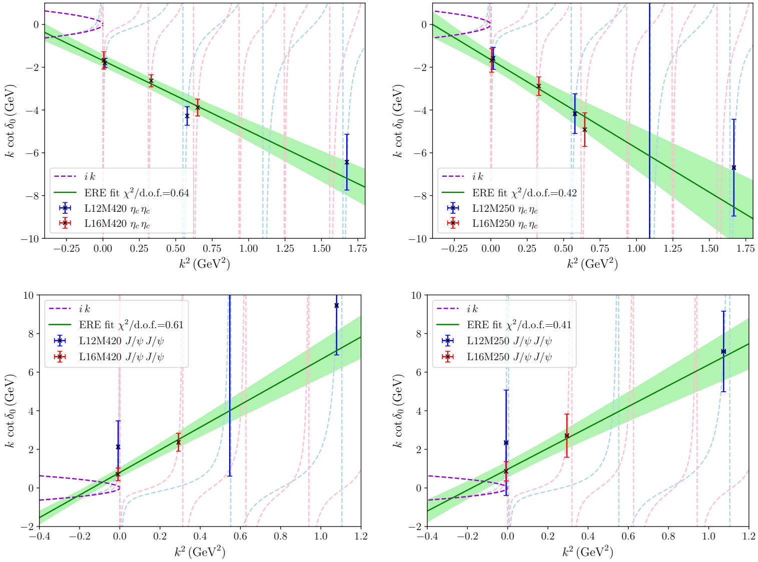

Figure 10: Scattering amplitudes ($k\cot\delta_0(k)$) for the 0^{++}system of $\eta_c\eta_c$ (upper) and $J/\psi J/\psi$ (lower).

0^{++} single-channel $\eta_c\eta_c$ scattering

- For low-energy scatterings, the phase $k\cot\delta_0(k)$ is parametrized by effective range expansion (ERE), where a_0 is the S-wave scattering length and r_0 is the effective range.

$$k\cot\delta_0(k) = \frac{1}{a_0} + \frac{1}{2}r_0 k^2 + \mathcal{O}(k^4),$$

- By fitting ERE , the scattering length a_0 and effective range r_0 for $\eta_c\eta_c$ system,

$$\text{M420} : a_0 = -0.117(19)\ \text{fm},\ \ r_0 = -1.30(20)\ \text{fm},$$
$$\text{M250} : a_0 = -0.120(26)\ \text{fm},\ \ r_0 = -1.63(40)\ \text{fm}.$$

  A lattice QCD study[7] calculates the low-energy S-wave $\eta_c\eta_c$ scattering at zero relative momentum and obtains a similar scattering length $a_0^{0^{++}} = -0.104(9)$ in the continuum limit.

- The negative value of a_0 indicates a repulsive interaction in $^1S_0$ $\eta_c\eta_c$ system, as we have seen that the $\eta_c\eta_c$ energies near the threshold are higher than the non-interacting energies.
- Our analysis shows no indication of additional structures in the $^1S_0$ $\eta_c\eta_c$ channel.

[7] Eur.Phys.J.C 85 (2025) 4, 458

0^{++} single-channel $J/\psi J/\psi$ scattering

- In $J/\psi J/\psi$ system, the a_0 and r_0 are

$$\text{M420}: a_0 = 0.25(7)\,\text{fm}, \quad r_0 = 2.31(33)\,\text{fm},$$
$$\text{M250}: a_0 = 0.20(8)\,\text{fm}, \quad r_0 = 2.14(41)\,\text{fm},$$

- By solving the pole equation with ERE parameterization

$$k \cot\delta(k) = i\,k.$$

- A virtual state below the $J/\psi J/\psi$ threshold by 28(10) MeV at $m_\pi = 420$ MeV and 38(20) MeV for $m_\pi = 250$ MeV. An near-threshold enhancement in the production cross-section.

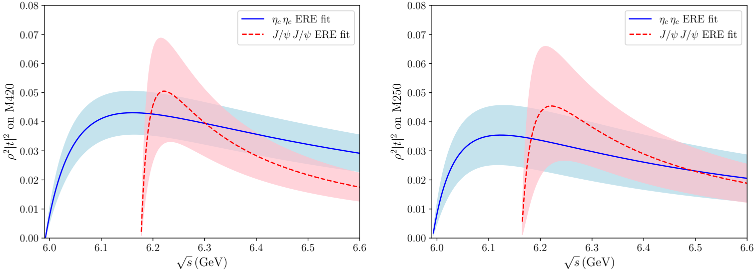

Fitted energy level spectrum

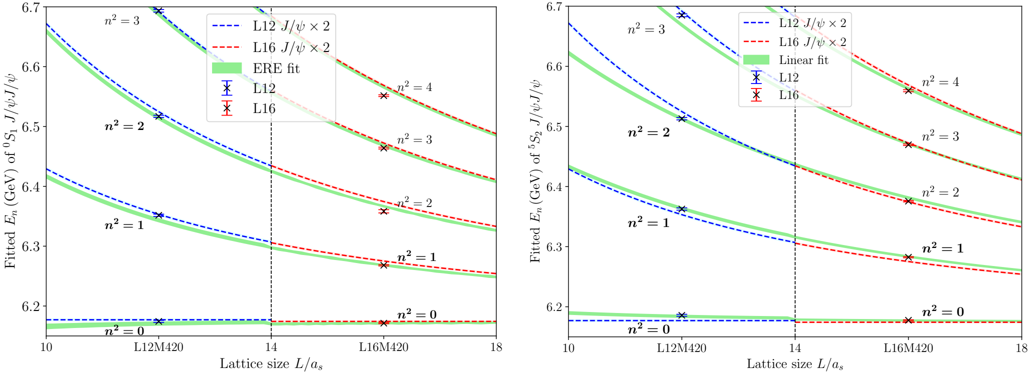

Figure 11: Fitted energy level spectrum for 0^{++} and 2^{++} system.

Energy levels for 0^{++}

Table 1: Energy levels (in GeV): E_n (complete operators set), E'_n (only $\eta_c\eta_c$), and E''_n (only $J/\psi J/\psi$).

E_n	L12 non-int	L12 E_n	L12 E'_n	L12 E''_n	L16 non-int	L16 E_n	L16 E'_n	L16 E''_n
				$m_\pi = 420$ MeV				
E_1	5.9919(13)	**5.9966(13)**	5.9965(13)	-	5.9905(7)	**5.9925(7)**	5.9926(7)	-
E_2	6.1726(17)	**6.1820(15)**	6.1840(16)	-	6.0938(9)	**6.1001(7)**	6.1003(7)	-
E_3	6.1770(17)	**6.1743(17)**	-	6.1721(16)	6.1743(10)	**6.1713(9)**	-	6.1715(9)
E_4	6.3481(21)	**6.3512(15)**	6.3566(16)	-	6.1954(11)	**6.2039(7)**	6.2033(7)	-
E_5	6.3532(22)	**6.3516(19)**	-	6.3343(18)	6.2752(13)	**6.2681(11)**	-	6.2544(14)
E_6	6.5188(24)	**6.5270(17)**	6.5262(17)	-	6.2954(14)	6.3018(8)	6.3000(8)	-
E_7	6.5247(27)	**6.5169(18)**	-	6.5012(19)	6.3745(16)	6.3583(27)	-	6.3382(16)
E_8	6.6852(27)	6.6742(15)	6.6743(35)	-	6.3906(12)	6.3908(10)	6.3901(10)	-
E_9	6.6918(31)	6.6933(22)	-	6.6743(22)	6.4724(18)	6.4539(15)	-	6.4399(20)
E_{10}	6.8549(36)	6.8374(22)	-	6.8161(24)	6.5687(21)	6.5515(15)	-	6.5225(24)
				$m_\pi = 250$ MeV				
E_1	5.9913(14)	**5.9968(20)**	5.9958(26)	-	5.9966(7)	**5.9987(7)**	5.9987(7)	-
E_2	6.1714(18)	**6.1811(20)**	6.1831(33)	-	6.0996(10)	**6.1057(8)**	6.1058(8)	-
E_3	6.1633(20)	**6.1608(25)**	-	6.1575(25)	6.1706(10)	**6.1680(9)**	-	6.1674(10)
E_4	6.3464(22)	**6.3448(21)**	6.3543(40)	-	6.2009(14)	**6.2080(9)**	6.2077(10)	-
E_5	6.3406(24)	**6.3445(27)**	-	6.3228(31)	6.2714(14)	**6.2652(16)**	-	6.2539(15)
E_6	6.5167(26)	**6.5246(24)**	6.5235(27)	-	6.3005(17)	6.3053(11)	6.3036(11)	-
E_7	6.5130(28)	**6.5025(26)**	-	6.4931(24)	6.3706(18)	6.3578(36)	-	6.3422(20)
E_8	6.6827(30)	6.6692(24)	6.6706(22)	-	6.3986(20)	6.3945(14)	6.3934(12)	-
E_9	6.6810(32)	6.6805(25)	-	6.6644(28)	6.4682(22)	6.4600(31)	-	6.4445(24)
E_{10}	6.8449(36)	6.8206(30)	-	6.7996(38)	6.5645(25)	6.5429(39)	-	6.5287(26)

Energy levels for 2^{++}

Table 2: Energy levels (in GeV): E_n (complete operators set), E'_n (only $\eta_c\eta_c$), and E''_n (only $J/\psi J/\psi$).

E_n	L12 non-int	L12 E_n	L12 E'_n	L12 E''_n	L16 non-int	L16 E_n	L16 E'_n	L16 E''_n
				m_π = 420 MeV				
E_1	6.1726(17)	**6.1757(14)**	6.1761(14)	-	6.0938(9)	**6.0954(7)**	6.0952(7)	-
E_2	6.1770(17)	**6.1858(17)**	-	6.1863(17)	6.1743(10)	**6.1766(9)**	-	6.1774(9)
E_3	6.3481(21)	**6.3556(15)**	6.3553(16)	-	6.1954(11)	**6.1985(7)**	6.1984(7)	-
E_4	6.3532(22)	**6.3626(20)**	-	6.3626(20)	6.2752(13)	**6.2824(10)**	-	6.2822(10)
E_5	6.5247(27)	**6.5129(20)**	-	6.5121(21)	6.3745(16)	6.3757(12)	-	6.3757(12)
E_6	6.6852(27)	6.6792(19)	6.6792(19)	-	6.3906(12)	6.3934(8)	6.3930(8)	-
E_7	6.6918(31)	6.6849(24)	-	6.6849(24)	6.4724(18)	6.4701(11)	-	6.4695(13)
E_8	6.8549(36)	6.8410(20)	-	6.8391(22)	6.5687(21)	6.5602(13)	-	6.5592(15)
				m_π = 250 MeV				
E_1	6.1714(18)	**6.1737(37)**	6.1737(37)	-	6.0996(10)	**6.1004(8)**	6.1004(8)	-
E_2	6.1633(20)	**6.1730(26)**	-	6.1730(26)	6.1706(10)	**6.1736(10)**	-	6.1736(10)
E_3	6.3464(22)	**6.3523(40)**	6.3525(39)	-	6.2009(14)	**6.2030(9)**	6.2029(9)	-
E_4	6.3406(24)	**6.3509(37)**	-	6.3508(37)	6.2714(14)	**6.2791(15)**	-	6.2790(14)
E_5	6.5130(28)	**6.5026(21)**	-	6.5026(21)	6.3706(18)	6.3718(20)	-	6.3719(17)
E_6	6.6827(30)	6.6745(20)	6.6745(20)	-	6.3986(20)	6.3967(13)	6.3966(11)	-
E_7	6.6810(32)	6.6743(20)	-	6.6743(20)	6.4682(22)	6.4657(14)	-	6.4656(14)
E_8	6.8449(36)	6.8246(20)	-	6.8223(25)	6.5645(25)	6.5543(27)	-	6.5551(19)

2^{++} single-channel $J/\psi J/\psi$ scattering

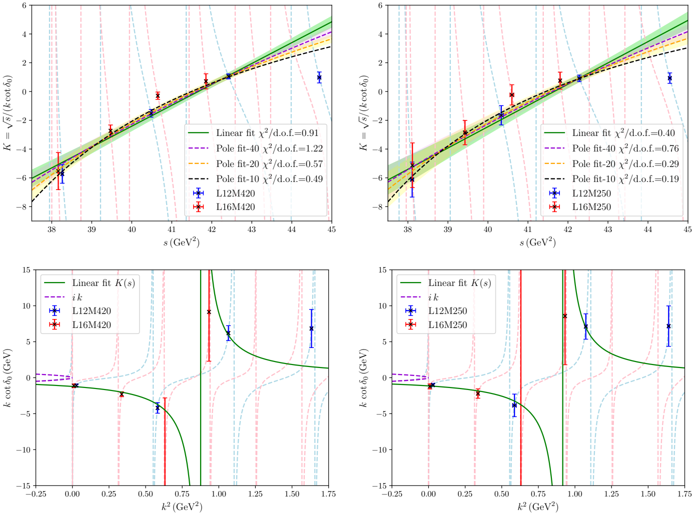

Figure 12: The $K(s)$-matrix and $k\cot\delta$ for the 2^{++} $J/\psi J/\psi$ channel, obtained using various fit parameterizations at two different pion masses.

2^{++} single-channel $J/\psi J/\psi$ scattering

- In low-momentum region, the ERE has

$$\text{M420}: a_0 = -0.163(16)\ \text{fm},$$
$$\text{M250}: a_0 = -0.171(29)\ \text{fm}.$$

  In Ref the scattering length in the continuum limit is given as $a_0^{2^{++}} = -0.165(16)$ fm.

- Based on the distribution of the data points, a linear fit (green line) is naturally adopted, and for comparison, we also consider the widely used sum-of-poles parameterization model

$$K(s) = a\,s + b, \quad K(s) = \frac{g^2}{m_0^2 - s} + \gamma.$$

  Due to overfitting in the pole model with three parameters, the fitting results are sensitive to the initial value of g (three examples are shown as purple, orange, and black lines). When $g \longrightarrow \infty$, these two models become equivalent.

- By solving the pole equation of the t-matrix

$$t^{-1}(s) = K^{-1}(s) - i\rho = 0,$$

  three complex pole solutions are obtained.

Phase shift

Note that the zero of $K(s)$ also gives the so-called CDD zero of the scattering amplitude t by

$$t(s) = \frac{K(s)}{1 - i\rho(s)K(s)}, \qquad t(s) \approx \frac{c_0^2}{s_0 - s},$$

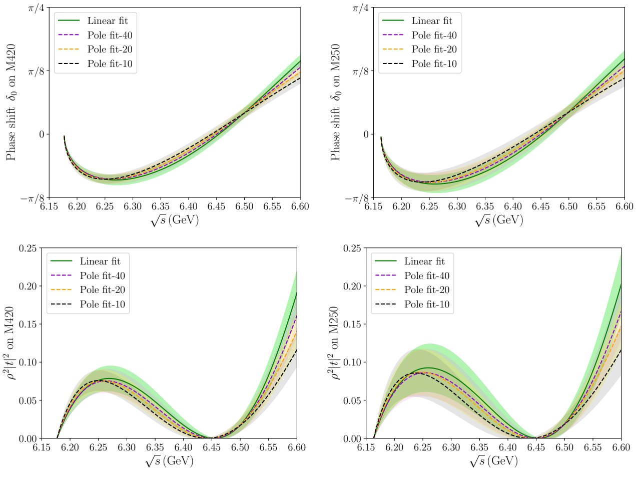

Pole position

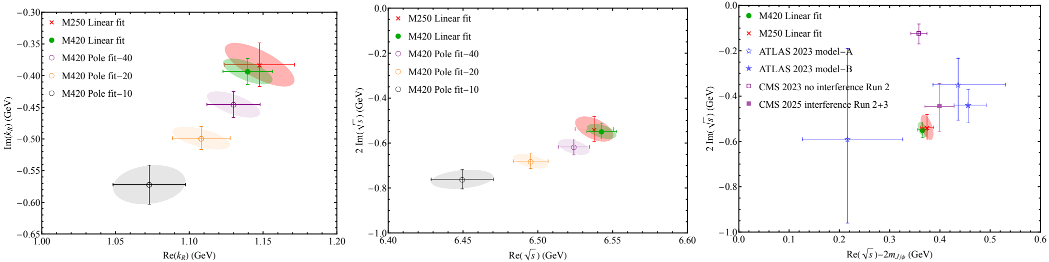

Figure 13: Pole positions located on Riemann Sheet II, analyzed using principal component analysis (PCA), in both the complex k-plane and $\sqrt{s}$-plane.

Parameters

Table 3: The K-matrix fitting parameters and the properties of the resonance (R) in $J/\psi J/\psi$ scattering, where $\hat{g} \equiv |c_0|/m_R$.

Parameters	Pole fit-10 M420	Pole fit-20 M420	Pole fit-40 M420	**Linear fit M420**	**Linear fit M250**
g_0 (GeV)	11.5(1.5)	18.8(1.2)	38.6(0.7)	-	-
m_0^2 (GeV^2)	31.0(1.3)	24.9(1.4)	8.3(1.8)	-	-
γ	12.5(1.8)	21.3(1.2)	44.9(1.0)	-	-
a (GeV^{-2})	-	-	-	1.45(12)	1.48(20)
b	-	-	-	-60.4(4.9)	-61.6(8.4)
Re (k_R) (GeV)	1.073(25)	1.108(20)	1.130(18)	1.140(17)	1.148(24)
Im (k_R) (GeV)	-0.572(31)	-0.499(18)	-0.446(21)	-0.393(20)	-0.383(34)
m_R (GeV)	6.449(21)	6.495(12)	6.524(11)	6.543(10)	6.538(13)
Γ_R (GeV)	0.761(42)	0.681(32)	0.617(35)	0.548(34)	0.537(56)
$\|c_R\|^2$ (GeV^2)	22.2(1.0)	19.7(0.5)	18.0(0.6)	16.2(0.6)	15.9(1.1)
$\|c_R\|$ (GeV)	4.71(10)	4.39(6)	4.44(6)	4.02(8)	3.99(14)
$\Gamma_{J/\psi J/\psi}$ (GeV)	0.494(19)	0.469(17)	0.443(19)	0.408(19)	0.406(31)
$\mathrm{Br}_{J/\psi J/\psi}$	65(2)%	69(2)%	72(2)%	74(2)%	75(3)%

Summary and outlook

Summary and outlook

- First results on $\eta_c\eta_c$ and $J/\psi J/\psi$ scattering spectrum from lattice QCD;
- Couple channel effects are weak between $\eta_c\eta_c$ and $J/\psi J/\psi$;
- For 0^{++} $\eta_c\eta_c$, repulsive interaction (no structure);
- For 0^{++} $J/\psi J/\psi$, a virtual state in ${}^1S_0$ channel, an enhancement near 6.2 GeV;
- For 2^{++} $J/\psi J/\psi$, a resonance in ${}^5S_2$ channel, mass $\sim$ 6.54 GeV, width $\sim$ 540 MeV;
- All key steps have been cross-checked: two lattice volumes, two sea quark masses, and two methods for extracting energy levels, yielding consistent results;
- Completely independently and almost simultaneously with CMS experiments: Agreement.
- Outlook: higher channels $J/\psi\psi'(6900?)$; $Z_c(3900)$; $X(3872)$...

Thanks!

Any questions, please?